Materials Physics and Mechanics 27 (2016) 113-117 Received: February 19, 2016

SIMULATION OF ELECTROMECHANICAL PROPERTIES OF ORDERED CARBON NANOTUBE ARRAYS

Viatcheslav Barkaline*, Aliaksandr Chashynski

Belarusian National Technical University, Nezavisimosti ave., 65, 220013 Minsk, Belarus

*e-mail: barkaline@bntu.by

Abstract. Phenomenological approach to frequency domain electric properties of ordered carbon nanotube arrays is presented accounting mechanical resonances of nanotubes. It is shown numerically that resonances could lead to strong frequency dependence of dielectric permittivity of arrays and UHF devices using them.

1. Introduction

The developing of the technology of selective deposition of oriented carbon nanotube (CNT) arrays seems one of the most promising achievements of modern nanotechnology [1]. Such arrays may consist of single wall and multiwall nanotubes with diameter from dozens to hundreds nanometers and lengths up to several micrometers and present an example of highly ordered dispersive medium with significant contribution of van der Waals interactions to all properties of the material.

Ordered CNT arrays are very promising in various nanotechnology applications such as chemical and biosensors, UHF devices. Due to the small dimensions of carbon nanotubes their individual mechanical resonances and resonances of their arrays fell into UHF and microwave regions [2]. Resonance behaviour of CNT arrays has to manifest itself in electrodynamical properties of arrays and, in particularly, in frequency dependence of dielectric permittivity.

2. Dielectric permittivity of CNT array

From the phenomenological viewpoint the interaction of electron and ion subsystems CNT could lead to the excitation of CNT vibration due to its polarization in electric field during which ponderomotive forces acting on CNT arise [3-4].

On the basis of classical dispersion theory with account of relaxation processes the dielectric permittivity of CNT array in this approximation can be represented as

$$\varepsilon_{ij}^{CNT}(\omega)=(1-\frac{4\pi ne^2}{m(\omega^2-i\omega\Gamma)})\delta_{ij}+\frac{3x^{(ij)}(\omega)}{3-x^{(ij)}(\omega)}+\frac{4\pi\sigma}{i\omega}\delta_{i3}\delta_{j3}, \quad (1)$$

where

$$x^{(ij)}(\omega)=\frac{4\pi e^2}{m}\sum_k\frac{N_k A_k^{(ij)}}{{\omega_k}^2-\omega_{Fk}^2-\omega^2+i\omega\Gamma_k}. \quad (2)$$

N_k - number of active charges for given mode per unit volume, n – free electrons' density, m – electron mass, e – electron charge, σ - specific electric conductivity of CNT, δ_{ij} - Kronecker's delta. Second term in (1) is caused by plasma oscillations of free electrons in electromagnetic field with attenuation Γ. The third term corresponds to induced vibrations of the array subsystems with eigenfrequencies ω_k and attenuations Γ_k. Oscillators correspond to these

subsystems are localized then the Lorentz correction $\omega_{Fk}^2 = 4\pi N_k e^2 F_k / m$ accounting local field could be essential for them, F_k is Lorentz factor. Contribution of static conductivity to imaginary part of dielectric permittivity along tubes (z axis direction) is taken into account by separate term. Phenomenological parameters $A_k^{(ij)}$, N_k and Γ_k account the excitation efficiency and resonant line width with the line central frequency ω_k. Nonzero Γ_k values are caused as by nanotubes' interaction in array as by variations of their geometry through the array. In quantum description $A_k^{(ij)}$ are proportional to corresponding oscillator strength.

We calculated eigenfrequencies in the region of 2.6-3.75 GHz for four configurations of CNT arrays in continual approximation. First configuration (a) is presented schematically in Fig. 1a and is composed from 23 nanotubes of outer and inner diameters 10 and 5 nanometers respectively and length 13.5 microns. Distances between CNT axes forming trigonal lattice was taken equal to 20 nm. The bottom and up of the array were formed by graphene-like layers of thickness 1 nm.

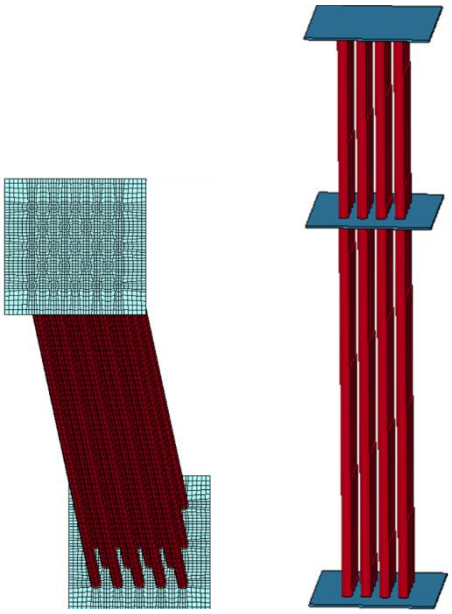

Fig. 1. Eigen mode frequencies versus mode number for sample CNT array.

Second and third configurations (b) and (c) are similar to (a) with nanotube lengths 27.5 and 67.2 microns correspondingly. Fourth configuration (d) is presented in Fig. 1b and consists of two CNT array layers with nanotube lengths 75 and 37 microns divided by additional graphene-like 1 nm layer. Elastic modules and mass density of nanotube material were calculated on molecular mechanics level of theory using approach described in [5]. For array in configuration (a) the finite element network contained 33338 nodes, and 1614 eigen modes are found for the frequency domain depicted (Fig. 2a). For configurations (b), (c), (d) 943, 1430, 3783 modes were found respectively. Figure 3 shows arrays 'eigenfrequencies' distributions for all configurations which are strongly non-uniform.

Then dielectric permittivity tensors (1) for arrays were calculated assuming that maximal N_k value corresponds to the density of carbon atoms multiplied by the number of valence electrons per atom:

$$\max\{N_k\} = 4\frac{N_c}{(D+a)^2 h}\frac{2}{\sqrt{3}}, \qquad (3)$$

where N_c - number of carbon atom in CNT, D - its diameter, a - minimal distance between CNT in array, h - CNT length.

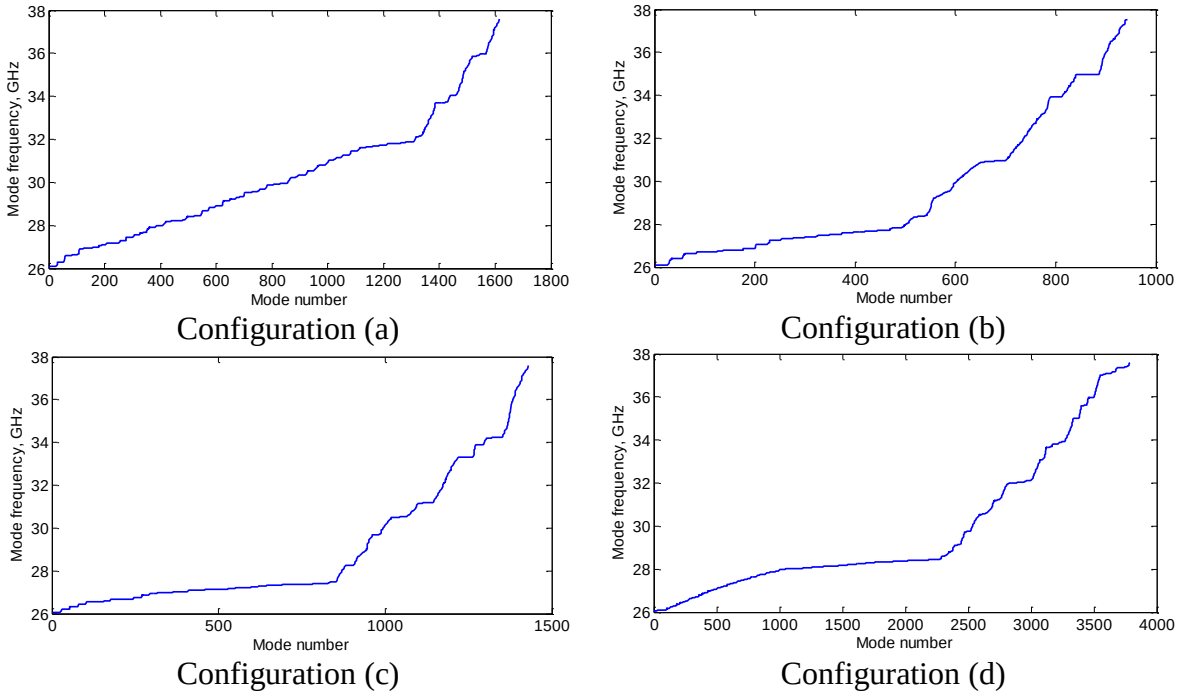

Fig. 2. Eigen mode frequencies versus mode number for CNT arrays in various configurations.

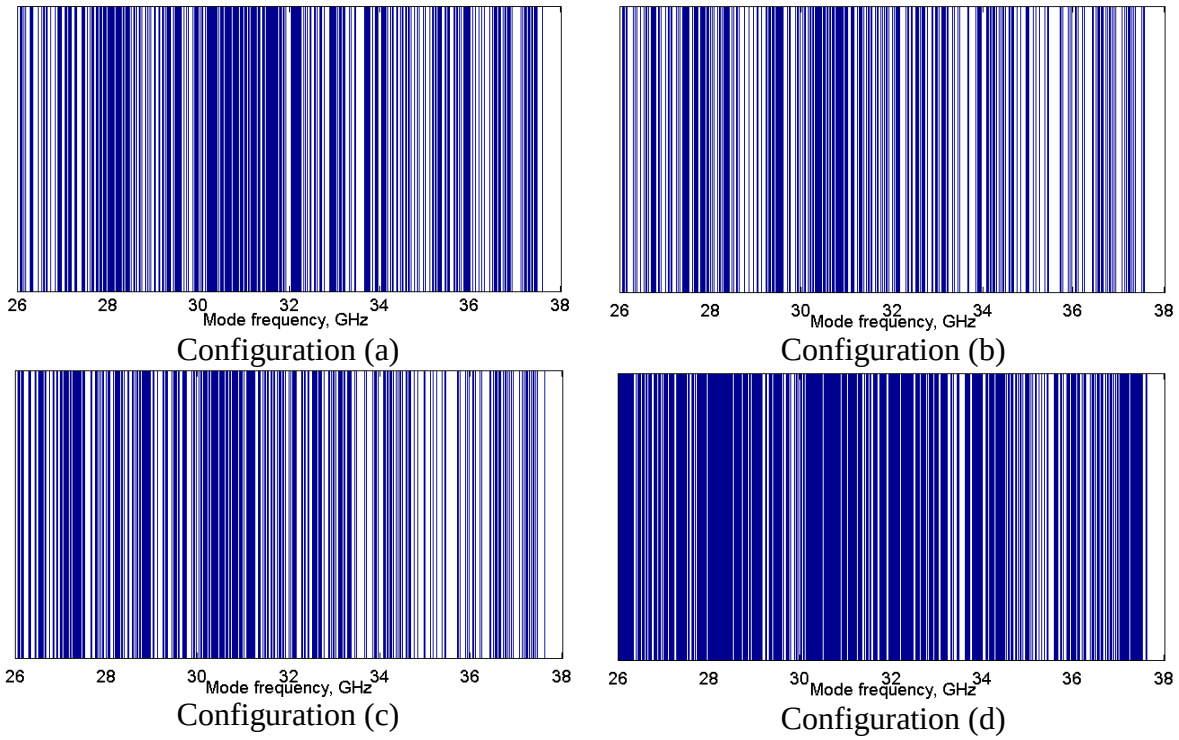

Fig. 3. Eigen frequencies' distribution for CNT arrays in various configurations.

Accounting of non-efficiency of excitation of electrons was made by efficiency parameter

$$\zeta = \frac{N_k}{\max\{N_k\}}. \tag{4}$$

The fact that the material of CNT does not fill whole volume of the array could be taken into account in the effective media approximation, which gives

$$(1-f)\frac{1-\varepsilon}{1+2\varepsilon}+f\frac{\varepsilon^{CNT}-\varepsilon}{\varepsilon^{CNT}+2\varepsilon}=0, \qquad (5)$$

where f - volume part of CNT material, $\varepsilon(\omega)$ - effective permittivity of array. ZZ-component of arrays' permittivities calculated from (5) are presented in Fig. 4. In calculation we set $A_k^{(ij)}=\delta_{ij}$, $\sigma=0$. One can see strong dispersion of real and imaginary parts of $\varepsilon_{ij}(\omega)$.

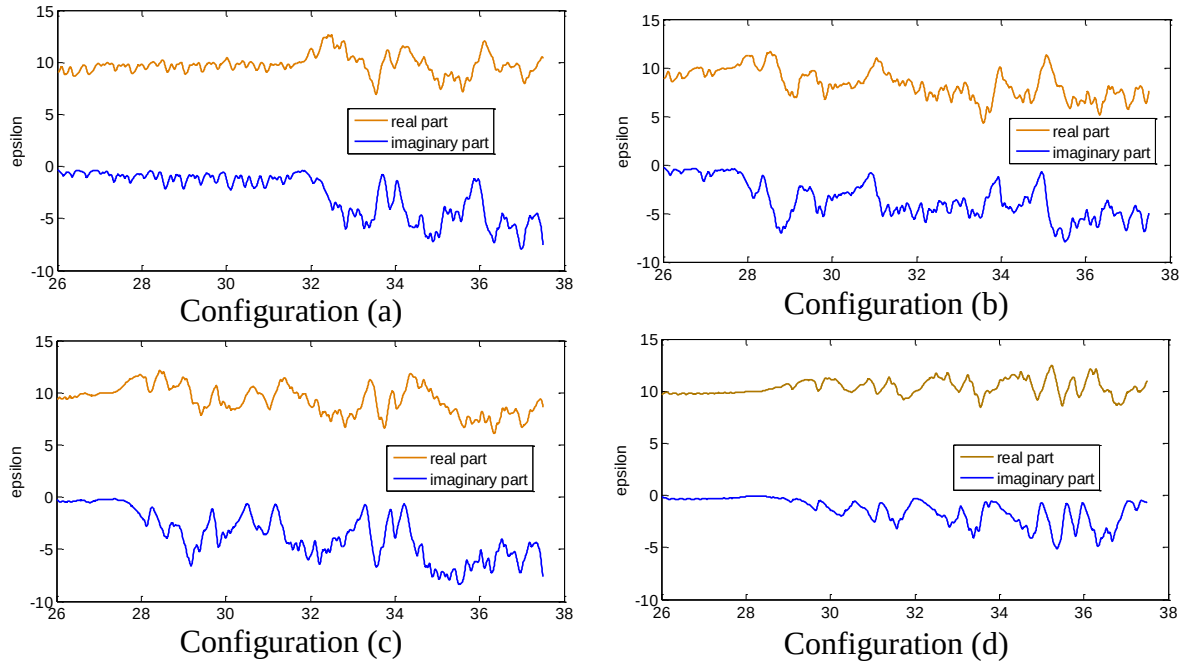

Fig. 4. Real and imaginary parts of $\varepsilon_{zz}(\omega)$ for CNT arrays in various configurations. Horisontal axis – frequencies in GHz, $\Gamma_k=0.5\cdot10^9$ Hz, $\zeta=0.1$.

3. UHF filter with CNT array insert

As an example of application of the frequency domain properties of CNT array we studied the UHF filter with CNT array insert. The construction of the filter is presented in Fig. 5. It consist of resonant metal cavity with CNT array insert which divides cavity by two equal parts and input and output metal waveguide lengths.

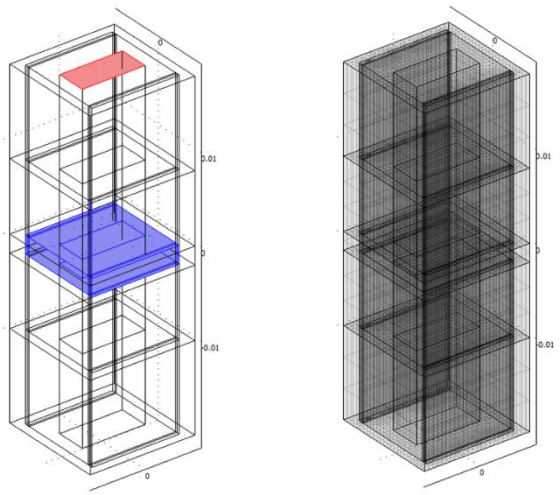

Fig. 5. The construction of UHF filter with CNT array insert, input port and insert are colored, dimensions in m. Finite element mesh of construction, number of degrees of freedom 549974, number of nodes 24531, number of elements 22326.

Calculated frequency dependences of S11 and S21 parameters of UHF filter with CNT array insert are shown in Fig. 6 and 7.

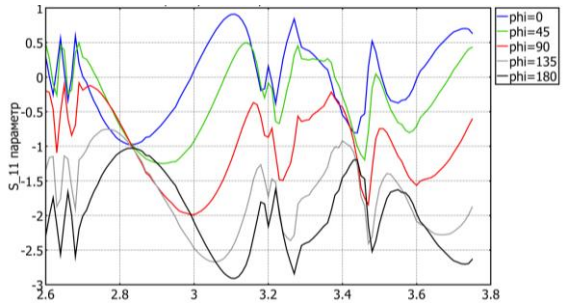

Fig. 6. Frequency dependence of S11 parameter of UHF filter with CNT anisotropic array insert for various phase of a signal. Frequencies are shown along X-axis in tens of GHz.

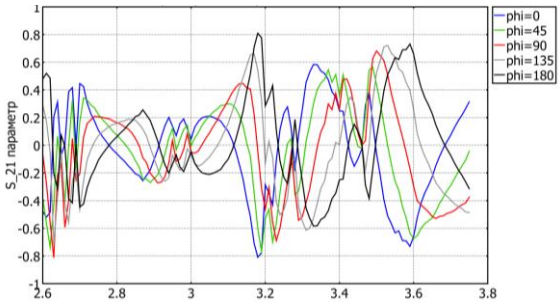

Fig. 7. Frequency dependence of S21 parameter of UHF filter with CNT anisotropic array insert for various phase of a signal. Frequencies are shown along X-axis in tens of GHz.

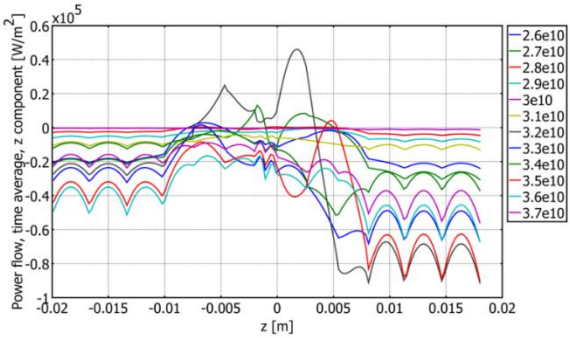

Fig. 8. Electromagnetic power flow on the filter axis for various frequencies shown in legend in GHz. Input power 1 W.

The frequency and coordinate dependence of longitudinal power flow at the axis of the filter is shown in Fig. 8. The data presented demonstrate that frequency dependence of CNT array permittivity defines the filter properties and could be determined in experiments with UHF technique.

4. Conclusion

Possible contribution of resonant mechanical vibration to frequency dependence of electromagnetic properties of ordered CNT arrays is estimated in UHF region and its experimental manifestation in UHF filter characteristics is discussed.

References

[1] A. Basaev et al, In: *Nanotechnology International Forum* 3-5.12, Moscow, 2008: Abstracts, Scientific and Technological Sections (Moscow, 2008), Vol. 2, p. 25.
[2] V. Barkaline, P. Zhuchak // *Proceedings of SPIE* **7377** (2009) 73770I.
[3] V. Barkaline, I. Abramov, E. Belogurov, A. Chashynski, V. Labunov, A. Pletezhov, Ya. Shukevich // *Nonlinear Phenomena in Complex Systems* **15(1)** (2012) 23.
[4] V. Barkaline, A. Chashynski, In: *Chemical Sensors: Simulation and Modeling*, ed. by G. Korotcenkov (Momentum Press, N.Y., 2012), Vol. 3, p. 289.